ELSEVIER

Surface Science 317 (1994) 15–36

surface science

Diffusion mechanisms relevant to metal crystal growth: Pt/Pt(111)

Marie Villarba, Hannes Jónsson *

Department of Chemistry, BG-10, University of Washington, Seattle, WA 98195, USA

Received 18 March 1994; accepted for publication 23 June 1994

Abstract

We have studied theoretically diffusion processes relevant to metal crystal growth, focusing on the Pt(111) system. Using an EAM-type potential function to describe the atomic interactions, we have determined minimum energy paths and evaluated activation energy barriers for various adatom hop and exchange diffusion mechanisms. We find a surprisingly wide range of activation energies for descent of adatoms from atop islands, with the energy barriers not scaling simply with the energy of the initial and final states. Short and irregular island edges can have an order of magnitude lower descent barriers than long, straight edges, primarily due to the presence of corner atoms. However, heptamers and smaller islands with only corner atoms at the island edge have very high barriers for descent. With this exception, our results support the hypothesis made earlier by Kunkel, Poelsema, Verheij and Comsa [Phys. Rev. Lett. 65 (1990) 733] that small and irregular islands provide lower barriers for adatom descent, which helps explain the observed *reentrant* layer-by-layer growth. We have also studied the approach of adatoms towards descending and ascending steps and find the adatom is in both cases attracted towards the step edge, resulting in trapping at low temperature.

1. Introduction

The growth of thin metal films has been studied for several decades and has recently received considerable attention with the advent of techniques, such as molecular-beam epitaxy and chemical vapor deposition, for growing extremely thin films [1]. These films can be developed with unique properties useful for a multitude of devices – electronic, superconducting, magnetic, optical, etc. Furthermore, the quest to obtain information faster, cheaper, and more efficiently results in a continual need for even smaller and more densely packed microelectronic devices. Good performance for many of these devices requires an orderly arrangement of atoms within the films. The ultimate goal is to optimize growing structures by controlling the motion of atoms during growth, and to accomplish this, a thorough understanding of the atomic-scale processes governing surface morphologies is required. Despite the many theoretical and experimental investigations of thin metal film growth, many fundamental questions remain unanswered, even for the simplest case: homoepitaxial growth.

* Corresponding author. Fax: +1 206 685 8665; E-mail: hannes@u.washington.edu.

SSDI 0039-6028(94)00384-L

The motivation for our study of diffusion processes on Pt(111) surfaces comes primarily from thermal energy He-atom scattering (TEAS) experiments by Poelsema and coworkers [2,3] and scanning tunneling microscopy (STM) experiments by Michely and coworkers [4]. In their TEAS experiments, Poelsema and coworkers [2,3] observe an intriguing temperature dependence in the Pt crystal growth. At high temperatures ($450 \lesssim T_s \lesssim 800$ K), they observe pronounced oscillations in the specularly reflected He-atom beam, a clear indication of layer-by-layer growth. At somewhat lower temperatures ($340 \lesssim T_s \lesssim 450$ K), a rapid and monotonic decay of the reflectivity was observed, indicating the onset of multilayer growth. Surprisingly, at still lower temperatures ($100 \lesssim T_s \lesssim 340$ K), oscillations are again observed, indicating the return to layer-by-layer growth. This kind of temperature dependence has been termed "reentrant" layer-by-layer growth and has subsequently been observed for other systems [5]. To explain the transition from multilayer growth to two-dimensional (2D) growth at low temperatures, Poelsema and coworkers [2,3] proposed the activation barriers for interlayer mass transport breakdown for small and irregular islands – sometimes referred to as the "barrier-breakdown" hypothesis. In STM experiments, Michely and coworkers [4] indeed observe small, dendritic islands in the low-temperature range but larger, compact islands at intermediate temperatures.

Layer-by-layer growth at remarkably low temperatures has also been noted in reflection high-energy electron diffraction (RHEED) experiments by Egelhoff and Jacob for Cu(100) [6] and in low-energy electron diffraction (LEED) from Pd(100) by Flynn, Evans, and Thiel [6]. Several explanations have been proposed for the observed 2D growth. Egelhoff and Jacob suggest that deposited atoms can use their latent heat of condensation to skip along the surface and form well-ordered layers. However, field-ion microscope (FIM) experiments by Wang and Ehrlich [7] on Ir(111) and computer simulations of metal-atom collisions with surfaces by Sanders and coworkers [8,9] and by Wang and Fichthorn [10] have shown that incident atoms are incorporated into the lattice close to the site of impact, at most two sites away. Evans et al. [11] have emphasized that pyramidal structures on the surface can funnel atoms down to their base, leading to a narrower distribution of growing layers. However, pyramidal structures would lead mostly to diffuse He-atom scattering, so this effect is insufficient to explain the high degree of specular reflectivity for He atoms from the Pt(111) surfaces in experiments by Poelsema and coworkers [2,3]. Using effective-medium theory (EMT), Stoltze and Nørskov [12] have carried out molecular dynamics (MD) simulations and barrier calculations for descent via hopping and exchange from small islands, particularly a trimer and heptamer, on a Cu(111) surface. Based on those results, they argue against the barrier-breakdown hypothesis. They emphasize the importance of another effect which can contribute to the reentrant layer-by-layer growth. In their simulation of vapor deposition of Cu on Cu(111) as well as in our simulations [13] and those of Wang and Fichthorn [10] of deposition of Pt on Pt(111), incoming vapor atoms directed atop islands have been observed to directly displace or "push-out" peripheral island atoms to become incorporated at the island edge. This can enhance layer-by-layer growth at low temperatures where islands are small and irregular, and there is a greater probability of incorporating impinging atoms in the growing layer. At the intermediate temperature range, where islands are large and compact, the push-out mechanism would be less effective. Ferrón [14] and Šmilauer, Wilby, and Vvedensky [15] have carried out Monte Carlo (MC) simulations where they emphasize the importance of such effects by letting atoms landing close to step edges descend to the lower level, while adatoms hopping over a descending edge (and even approaching the edge [15]) experience higher energy barriers than adatoms on a flat terrace. The push-out mechanism can, however, only be a small contributing factor to the reentrant layer-by-layer growth because islands are already too large well before coalescence is reached at the low temperatures where the reentrant oscillations are observed in the He-atom reflection [4,16].

In our previous molecular dynamics simula-

tions of vapor deposition of Pt atoms on the Pt(111) surface at 275 K using an EAM-type interaction potential, we found that remarkably well-ordered first and second layers are formed [13]. We identified several atomic-scale processes enhancing layer-by-layer growth. We observed push-out events but, because of the limited number of edge sites even at this low temperature and high flux, only ca. 20% of atoms deposited atop islands got incorporated into islands via push-out. For sufficiently long times between deposition events (> 100 ps), a larger fraction of atoms impinging atop islands get incorporated into the growing layer by thermally activated exchange descent, particularly at irregular island edges [13]. We present here calculations of a wide range of activation energy barriers for diffusion, in particular for the descent of adatoms from atop islands of various sizes and from step edges with kink sites. We use a powerful technique, the "nudged elastic band" method [17] to determine the minimum energy paths for the transitions and, thereby, evaluate the activation energy barriers. We find the descent barriers can be an order of magnitude lower for small and irregularly shaped islands compared with large, compact islands. Our results, therefore, provide evidence supporting the barrier-breakdown hypothesis of Poelsema and coworkers [2].

The EAM interaction potential is an empirical potential parametrized from various properties of the bulk crystal as well as the dimer [13]. Several groups have previously used EAM-type interaction potentials to estimate surface diffusion barriers. Liu, Cohen, Adams, and Voter calculated activation barriers for self-diffusion on several flat fcc metal surfaces and reported their values for comparison with available experimental data [18]. Kellogg and Voter have identified surface diffusion modes for Pt monomers, dimers and trimers on Pt(001) and obtained energy barriers in quite good agreement with field-ion microscope (FIM) experiments [19]. Liu and Adams, have evaluated activation energy barriers for vacancy diffusion and adatom diffusion at various Ni surfaces, including the descent of adatoms at straight edges [20]. More fundamental approaches to deriving the atomic interactions include the effective medium theory (EMT) of Nørskov and coworkers, which has been applied to estimate various diffusion barriers for Cu surfaces [12,21] including descent of adatoms from atop small clusters on Cu(111), and the corrected effective medium (CEM) theory of DePristo and coworkers, which has been applied to estimate diffusion barriers on various flat fcc (100) and fcc (111) surfaces [22]. Fully ab initio density functional calculations (DFT-LDA) of Al surface diffusion have been carried out by Feibelman for the flat Al(100) surface [23] and by Stumpf and Scheffler [24] for Al(111) flat and stepped surfaces, including descent of adatoms and the diffusion of adatoms along straight step edges. An EAM-type Al potential constructed in a way analogous to the Pt potential used here has been found to give barriers in good agreement with the ab initio calculations, in particular for exchange diffusion processes which are the central focus of the present study [25].

In the following sections, we present our calculated activation energy barriers for diffusion, focusing primarily on descent of adatoms from atop islands on the Pt(111) surface. We first give a brief summary of the theoretical techniques, including the "nudged elastic band" method and details of the system used in the calculations (Section 2). The next section gives a comparison of our calculated activation barriers for self-diffusion on various Pt surfaces with available experimental estimates as well as with barriers calculated by other groups using EAM and Morse potentials. We then present calculations of descent barriers for the two types of step edges on the (111) surface, including a detailed analysis of the effect of kink sites on the binding sites and descent barriers. We focus next on descent of an adatom from small islands and analyze how the energy barrier depends on island size. Finally, we look at the diffusion of an adatom towards ascending and descending steps.

2. Methodology

When diffusion can be described in terms of displacements of adatoms from one stable bind-

ing site to another, with the timescale of these displacement events being much longer than the vibrational motion, the diffusion rate can be approximated well with transition state theory (TST) [26–28]. The fundamental assumptions of transition state theory are (1) the transition rate is slow enough that a Boltzmann distribution is maintained in the "initial" or "reactant" state [26] and (2) a dividing surface can be found between the initial and final state which the system only crosses once (i.e. recrossings are neglected). If, furthermore, the vibrational motion is assumed to be harmonic, the expression for the rate, k^{TST}, of diffusive displacement simplifies to [28]

$$k^{\mathrm{TST}} = \nu_0 \, \mathrm{e}^{-E_a/k_B T}, \tag{1}$$

where ν_0 is the harmonic vibrational frequency (assuming just one vibrational mode here), typically on the order of 10^{13} s^{-1} in metallic systems. The activation energy, E_a, is the difference between the minimum energy of the system in the initial state, E_i, and the minimum energy of the system confined to a transition state, E_t

$$E_a = E_t - E_i. \tag{2}$$

Since TST neglects recrossings, the rate of escape from the initial state which is obtained from TST is an overestimate. The optimal dividing surface is therefore one that gives the lowest estimated rate. Within the approximation of Eq. (1), the optimal choice for the transition state is the highest energy configuration along a minimum energy path connecting the initial state and the final state. This configuration corresponds to a saddle point in the multidimensional potential energy surface. Within TST and the harmonic approximation, the problem is therefore reduced to searching through all possible paths between the initial and the final state and finding the maximum energy along the path. The lowest value for that energy barrier is the activation energy E_a that goes into the TST expression in Eq. (1).

Voter and Doll [28] have analyzed extensively the validity of TST and the corrections ("dynamical corrections") that can be applied to obtain the exact transition rate. For sufficiently high barriers and low temperatures ($E_a \gg kT_s$), where the probability of correlated multiple displacements is low, the dynamical corrections to transition state theory (TST) are small, as long as the transition state is chosen properly. Correlated displacements can lead to "bounce-back" trajectories which reduce the rate of escape and thereby result in less diffusion than predicted by TST. This effect has been observed in simulations of an adatom diffusing on the flat fcc (111) terrace of a Lennard-Jones crystal [29] as well as for metals [22]. Multiple jumps are another type of correlated displacements observed at sufficiently high temperatures. These lead to an underestimate of the diffusion coefficient in TST. Typically the errors in TST are much smaller than the uncertainty in the description of the energetics of the system. We will focus here on evaluation of the activation energy and assume Eq. (1) is an accurate enough estimate of the rate of escape. We are particularly interested in finding low energy pathways for atoms to descend from atop islands at very low temperature. In some cases we find very low barriers for which dynamical corrections are likely to be significant.

In order to identify the minimum energy path for a transition from a given initial state to a given final state without any previous knowledge of the transition state (such as a symmetry constraint), we have used the "nudged elastic band" method (NEB) [17]. This technique enables us to deal with low symmetry transitions involving displacements of several atoms. A path is constructed by creating several replicas of the full system with adjacent replicas held together by a harmonic restoring force. As a starting point, we have used a path that linearly interpolates the coordinates of the atoms in the initial and final states. As will be illustrated below, the path can change in a non-trivial way from the linear interpolation during an optimization procedure. In order to converge the path to the minimum energy path, an object function for the whole system of P images is defined as

$$F(R_1, \ldots, R_P) = \sum_{l=1}^{P} \left[V(R_l) + P_k (R_{l-1} - R_l)^2 \right], \tag{3}$$

with R_i representing all $3N$ coordinates of the N

atoms in the system. The object function is minimized with respect to the $3N(P-2)$ coordinates of the intermediate images $R_2, R_3, \ldots, R_{P-1}$. The first term is the energy of each image of the system calculated here with the EAM interaction potential. The second term represents the elastic restoring force with a spring constant that scales linearly with the number of images. That is, each atom in the system is turned into a chain of images of the atom, and adjacent images interact with a harmonic potential. Images of different atoms but corresponding to the same "link" in the chain, l, interact with each other through the EAM potential. In the limit of $P \to \infty$, the optimized path can be shown to coincide with the minimum energy path [17]. The convergence in P to the minimum energy path is accelerated by "nudging," in which elastic forces perpendicular and potential energy (EAM) forces parallel to the path are zeroed. This eliminates "corner cutting" and ensures that the images are evenly spaced in the $3N$-dimensional space. All activation barriers reported here have been calculated using the NEB method with $20 \leq P \leq 35$. The system used in the calculations consisted of between four to six layers, with roughly 90 to over 300 atoms per layer depending on the complexity of the process studied. The convergence of the optimization was measured in terms of residual forces on the atoms in the system. The minimization process was continued until the maximum force on every atom in the system had dropped below 10^{-5} eV/Å.

The EAM-type atomic interaction potential for Pt used here has the form

$$E_{\text{tot}} = \sum_{i>j} \phi(r_{ij}) + \sum_i F(\rho_i), \tag{4}$$

where ρ_i is the electron density at the site of atom i due to all the other atoms, F is the embedding energy, and $\phi(r_{ij})$ is the pair interaction between atoms i and j separated by a distance r_{ij}. Following Voter and Chen [30] the potential was fitted to estimated dimer energy and distance in addition to various bulk properties (cohesive energy, lattice constant, bulk modulus, elastic constants and vacancy energy) [31]. The function $\phi(r_{ij})$ was taken to be a Morse potential $\phi(r) = D(1 - e^{-\alpha(r-R)})^2 - D$ with depth D of 2.19 eV, a decay length α of 1.83 Å^{-1}, and reference position R of 2.35 Å. The density ρ_i is obtained by summing over "atomic electron densities" $\rho_i = \sum_{j \neq i} \rho^{\text{A}}(r_{ij})$ with $\rho^{\text{A}}(r) = r^6 (e^{-3.64\,\text{Å}^{-1} r} + 512\, e^{-7.28\,\text{Å}^{-1} r})$. Both ϕ and ρ are cut and shifted at 5.5 Å to make the interaction range finite. The embedding energy function, $F(\rho)$, is represented with a polynomial. The EAM potential includes many-body interactions between the atoms through the non-linearity of the embedding function. The forces used in the minimization procedure and in the molecular dynamics simulation are evaluated analytically.

In principle, all atoms in the system should be turned into chains in the NEB calculation, according to Eq. (3). However, the further away the

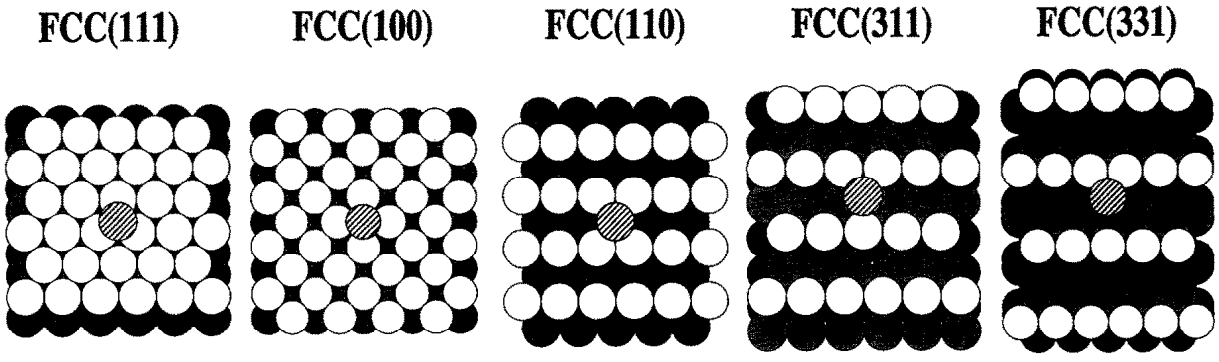

Fig. 1. Surface normal views for Pt surfaces where self-diffusion has been measured: (111), (100), (110), (311), and (331). The adatom sitting atop is shaded with stripes. Open circles denote atoms higher up than lightly shaded atoms, which in turn are above dark atoms.

chains are from the atoms displaced in the diffusion event, the more compact they are. For efficiency in the NEB calculation, only atoms within a certain radius (typically 7 Å) of the atom(s) displaced in the diffusion event are included as chains. Outside this "active region" the chains are forced to "collapse" into a single atom, i.e. chains outside the radius have all images at the same location, but this location can be different from the location of the atom in either the initial or final state. This greatly reduces the number of degrees of freedom in the minimization of the object function F. In the calculation of the EAM interaction, an image of a chain in the active region then contributes $\phi(r)/P$ to the pair interaction with atoms outside the active region and it contributes $\rho^{A}(r)/P$ to the electron density entering the evaluation of the embedding energy of atoms outside the active region. This approximation can be improved systematically by extending the radius of the active region so that chains near the boundary are compact enough for the approximation to be accurate.

3. Comparison with measured diffusion barriers

To get an idea of how well the EAM model for the atomic interactions describes the energetics of Pt surface diffusion, we have evaluated all Pt diffusion barriers for which experimentally measured values have been reported. Fig. 1 shows the views normal to five flat surfaces studied, (111), (100), (110), (311), and (331). Table 1 gives a comparison of the activation barriers calculated using our parametrization of the EAM-type potential. We point out that the potential is fitted only to various properties of the bulk crystal and the dimer. Since none of the diffusion barriers or any other surface property has been included in the fit, a different parametrization and different form for the EAM functions can lead to different values for the surface diffusion barriers. For comparison, Table 1 also includes barriers calculated by Liu et al. [18] using two other EAM-type potentials: one by Voter and Chen (VC) [30], very similar to our potential, and the other by Adams, Foiles, and Wolfer (AFW) [32] which has a different functional form and is not fitted to dimer properties. Also shown are activation energies calculated using a pairwise Morse potential [33].

A definitive experimental measurement of the diffusion barrier for a Pt adatom on the very smooth (111) surface has not been reported, but Bassett and Webber observed that adatoms were still mobile at temperatures as low as 77 K, indicating an activation barrier of less than 0.2 eV [33]. Estimates as low as 0.1 eV have been made [4], which would be in quite good agreement with the EAM calculation. An even smaller diffusion barrier (0.04 eV) has been reported on the basis of ab initio calculations of Al adatom diffusion on

Table 1
Comparison of activation energy barriers (reported in eV) for self-diffusion on various Pt surfaces, calculated using (1) our parameterization of an EAM-type potential, (2) an EAM potential by Voter and Chen (VC), (3) an EAM potential developed by Adams, Foiles and Wolfer (AFW), (4) a Morse potential by Basset and Weber, and (5) estimated experimentally using FIM by Kellogg and by Bassett and Webber

Surface	Our work	EAM (VC) [a]	EAM (AFW) [a]	Morse pot. [c]	Experimental
(111)	0.08	0.08	0.007	0.06	< 0.2 [b]
$(100)_{exch}$	0.54	0.64	0.31	3.75	0.47 ± 0.1 [d]
$(110)_{\parallel}$	0.46	0.53	0.25	0.53	0.84 ± 0.1 [b]
$(110)_{\perp exch}$	0.58	0.68	0.43	0.63	0.78 ± 0.1 [b]
(311)	0.57	0.63	0.43	0.49	0.69 ± 0.2 [b]
(331)	0.53	0.54	0.28	0.71	0.84 ± 0.1 [b]

[a] Liu, Cohen, Adams and Voter [8].
[b] Bassett and Webber [33].
[c] Calculated using Morse potential with parameters for Pt given in Ref. [33].
[d] Kellogg and Feibelman [34,35].

Al(111) [24]. These barriers are low because the adatom is unable to penetrate much into the close packed layer of surface atoms.

Self-diffusion on Pt(100) has been studied extensively by Kellogg and Feibelman [34,35] using FIM. Surprisingly, the adatoms were found to diffuse via an exchange mechanism rather than hops. The map of sites visited by the migrating Pt atom on the Pt(100) surface shows displacements only in the [100] and [010] directions of the substrate plane, consistent with a concerted-displacement mechanism where exchanging atoms maintain coordination with neighboring atoms. Our calculated activation energy for the exchange diffusion process is 0.54 eV, slightly higher but within the error estimate of the experimental value of 0.47 ± 0.1 eV. Kellogg estimated the Arrhenius prefactor for the exchange diffusion process and obtained a value of 1.3×10^{-3} cm^2/s, very similar to typical values for diffusion hop mechanisms [35]. As we show below, such exchange mechanisms are of central importance in low energy pathways for descent of adatoms from atop islands.

To illustrate the importance of the many-body interactions in the EAM potential, we have also calculated the activation energy barrier for exchange diffusion on the (100) surface using only a pairwise Morse potential with parameters provided by Bassett and Webber [33,36]. While many of the other diffusion barriers are predicted quite well with this potential, the energy barrier for the exchange diffusion on (100) is predicted to be 3.75 eV, an order of magnitude too large. This illustrates clearly that it is essential to include the many-body interactions present in the EAM potential. Given the good agreement between the calculated and measured activation energies for the diffusion on the (111) terrace and this exchange diffusion process, we expect that the various energy barriers presented below on adatom descent from islands of various shapes are at least showing the correct qualitative trends in the dependence of the activation barrier on the local environment.

For diffusion along channels, such as the diffusion on the (110), (311), and (331) surfaces, we obtain less satisfactory agreement with the experimental estimates [33]. We get reasonable agreement for the (311) surface but much lower barriers for the (331) and (110) surfaces than reported from the experiments. Both VC and AFW potentials give similarly low barriers for in-channel diffusion although the VC values generally get better agreement with experiment, as shown in Table 1. The EAM potential allows for large relaxation of the channel atoms during the diffusion process, which leads to channel widening when the adatom moves from its initial position to the transition state, amounting to 0.59 and 0.48 Å for the (110) and (331) surfaces, respectively. The Morse potential gives rise to smaller channel widening, 0.50 and 0.36 Å for the (110) and (331) surfaces, respectively.

The (311) consists of narrow terraces with A-type edges, while the (331) surface consists of narrow terraces with B-type edges. The diffusion barrier on these surfaces can therefore be expected to be similar to diffusion barriers along straight island edges. We have calculated the edge diffusion barriers to be 0.60 and 0.43 eV for the A- and B-type edges, respectively, as compared with 0.57 and 0.53 eV for the comparable (311) and (331) faces. Clearly the small size of the terraces does influence the relaxations of the atoms and thereby the diffusion barriers. Unfortunately, no direct measurement is available of the edge diffusion barriers, but we expect the values calculated with the EAM potential to be too low, in analogy with the other barriers for diffusion along channels.

For cross-channel diffusion on the (110) surface, a much lower barrier is obtained with an exchange mechanism (reported in Table 1 as $(110)_{\perp,\mathrm{exch}}$) as opposed to hopping, as suggested by Bassett and Webber [33]. This is also true for the Morse potential.

Thus, the activation energy barriers calculated using our EAM-type potential agree well with some of the available experimental data for self-diffusion on Pt surfaces. There is, however, a clear discrepancy in some cases, mostly where the adatom hops along a channel. It is unclear where this discrepancy comes from. Possibly channel-widening is too easy when the interaction is described with the EAM form. We emphasize that

we get good agreement between barriers predicted by our EAM potential and experiment for the processes most relevant to this study, diffusion on the (111) surface and the exchange diffusion processes on the compact (100) surface. In the present study, we focus on exchange diffusion at steps and kink sites with the goal of exploring the qualitative dependence of the descent barrier on the size and shape of islands.

4. Exchange descent at steps and kinks

The descent of adatoms from atop islands by a simple hop over the edge has a large energy barrier because the adatom loses coordination at the step edge. We have calculated values ranging from 0.7 to 0.8 eV depending on the local environment. An exchange mechanism where the adatom replaces an edge atom which in turn moves outwards from the edge has much lower energy barriers [13]. We have calculated activation barriers for exchange descent on the (111) surface at the two types of step edges, known as type A and B – the {100} and {111} faceted edges, respectively. We find a surprisingly wide range of exchange descent barriers depending on the type of edge and presence of kink sites.

4.1. Straight steps

Fig. 2a gives an illustration of the two types of stable step edges on the (111). The type A step has an underlying atom directly in front of each edge atom, but underlying atoms at a type B step provide a channel by which edge atoms can move directly away from the edge. The sites (numbered 1–10) correspond to positions on the energy curves plotted in Fig. 2b. The solid curves represent the energy for an atom to approach a step and descend via an exchange process. It is obtained by repeated application of the NEB method to trace the minimum energy path between the sites. The dashed curves, given as a reference, represent the energy for an atom to diffuse atop a large, flat terrace. There is a small difference in binding energy between fcc and hcp sites on a flat terrace, with the hcp site being

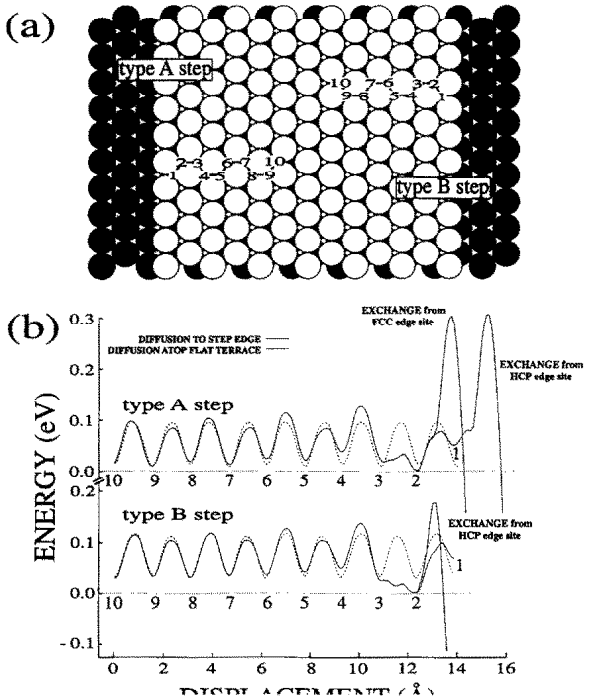

Fig. 2. (a) Illustration of the two types of step edges, A and B, for a large island. Sites along a general path that an adatom can take to approach a descending step are numbered from 1 to 10. (b) The dashed curves (given as a reference) correspond to the energy for an atom to diffuse atop a flat terrace. The solid curves represent the minimum-potential-energy profile for an adatom to hop from site 10 to site 1 then undergo exchange descent at the two types of edges. An adatom atop a type A step can undergo exchange from either fcc or hcp edge sites (sites 2 or 1), whereas exchange descent at a type B step always originates with the adatom atop at a hcp edge site (site 2, see text). The binding energy at the edge sites is particularly large because of the under-coordination of the edge atoms.

energetically favored by 7 meV. This is consistent with FIM experiments by Wang and Ehrlich [42] for Ir atoms on Ir(111). An interesting aspect of the curve for the approach to the step edge is the near disappearance of a barrier to hop from the center into edge sites (site 3 to site 2) and a general lowering of the binding energy at the edge. This is discussed futher in Section 6.2. Here we focus on the barrier for descent of an adatom via exchange.

At the type A step, an atom in the layer below sits directly in the way of an outgoing edge atom, impeding the edge atom from being displaced

normal to the step. In the exchange process, the displaced edge atom must move around the underlying atom, pushing against one of the edge atoms on either side of it. Fig. 3 shows the position of the atoms both in the initial state and at the transition state, where the energy is maximal along the transition path – i.e. the most difficult part of the transition. In order for the

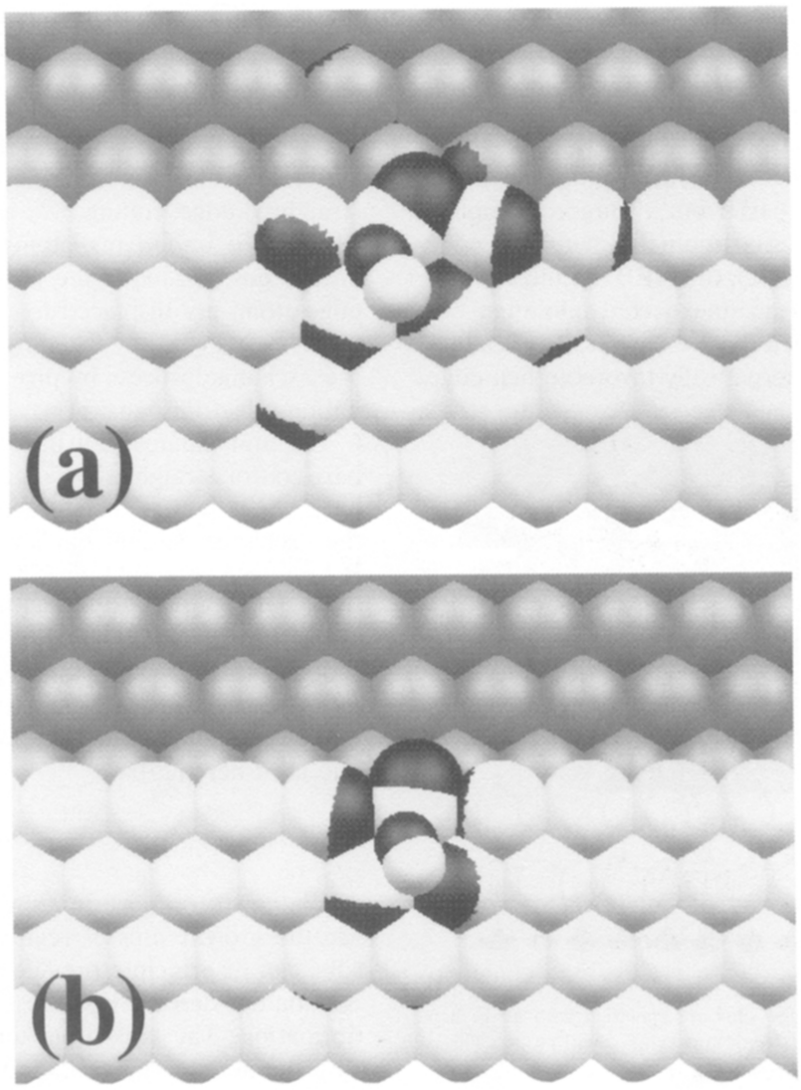

Fig. 3. Location of the atoms in the relaxed initial position (indicated by white spheres) and in the transition state corresponding to maximum energy configuration along the minimum energy path (black spheres) for the exchange descent process. The radius for spheres representing the adatom has been reduced to allow a more complete view of displacements of the underlying atoms. The spheres corresponding to the transition state have slightly smaller radius than spheres corresponding to the initial state. Therefore, for atoms with only minute displacement, only the initial state is visible. The larger the displacement, the more the black spheres become visible. Atoms in the underlying layer are represented by gray spheres. (a) For the type A step, an underlying atom sits directly in front of the exchanging edge atom, blocking it from moving directly outwards in the exchange process. The edge atom pushes against the adjacent edge atom to the right in the transition state and several other atoms show large displacement, including two lower layer atoms. (b) For the type B step, the underlying atoms provide a channel for the edge atom to move directly away from the step edge. Adjacent edge atoms are displaced *towards* the exchanging atoms, which facilitates and lowers the energy barrier for the exchange process.

displaced edge atom to move away from the edge, an adjacent edge atom has to move out of the way. The two adjacent edge atoms are displaced by 0.25 and 0.03 Å. Consequently, the barrier for exchange descent at this type of edge is rather high, 0.30 eV from an fcc edge site and 0.25 eV from a hcp edge site. The hcp edge site (labeled 1 in Fig. 2) is higher in energy than the fcc edge site (labeled 2) by ~ 0.05 eV which accounts for the difference in the descent barriers.

We find exchange descent from the type B straight edge to be easier but also more complex. When the adatom sits originally in an fcc edge site (labeled 1 in Fig. 2), the NEB optimization of the path results in an unexpected minimum energy path, involving a double barrier. The adatom first hops to the energetically favorable hcp edge site (site 2 in Fig. 2) before undergoing exchange. The hcp site is lower in energy by ~ 0.07 eV. We emphasize that there is no bias in the initial setup of the NEB calculation for this, the initial path involves simply a straight line interpolation of the initial and final configuration of atoms and therefore does not go close to the hcp site. The energy barrier for exchange from the hcp edge site is quite low, 0.18 eV. The process is much easier at this type of step because the displaced edge atom can easily move in a direction normal to the straight B edge, rolling over a bridge site formed by the two underlying atoms. At the maximum energy position along the path, the two adjacent edge atoms are displaced *towards* the exchanging atoms (see Fig. 3) by 0.26 and 0.10 Å, facilitating the exchange process by providing added coordination (electron density).

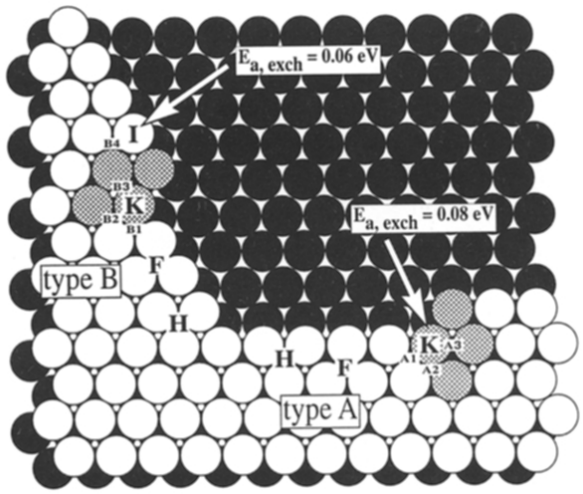

Fig. 4. Illustration of the kink sites on the two types of step edges, A and B. fcc edge sites are specified with an F, hcp edges sites with an H, and kink atoms with a K. Three possible initial starting positions for an adatom undergoing exchange diffusion with a type A kink atom are shown as A1, A2, and A3. An adatom at A3 sits in a near fourfold-coordinated site, created by the relaxations of the four shaded atoms below. Similarly, some initial starting positions for an adatom atop a type B kink site are shown as B1, B2, B3 and B4. B3 represents a near fourfold-coordinated site, formed by the four shaded atoms. The barrier for an adatom to descend by exchange with a kink atom, K, at type A edge (indicated with an arrow) is only 0.08 eV. At a type B kink, an adatom can descend by exchange with atom I (indicated with an arrow). The activation energy barrier for this process is only 0.06 eV but the displaced edge atom ends up having low coordination.

Liu and Adams [20] have calculated descent barriers for straight step edges on Ni(111), using an EAM potential. They also note an increase in the exchange descent barrier in going from type B to type A straight steps. Stumpf and Scheffler [24] carried out density-functional calculations for steps on the Al(111) surface and got a similar ratio between the two barriers, although the magnitudes are much smaller (as predicted by an EAM-type interaction potential similar to the one used here [25]).

4.2. Kink sites

We now turn our attention to kink sites, which are the growth sites of regular step edges. Kink sites can in principle provide lower energy paths for adatom descent because of the increased coordination. The kink atom undergoing exchange with the adatom is designated with a K in Fig. 4. Here the relaxation of the edge atoms has a more dramatic effect than at the straight edge. An adatom placed in either of the two sites near A3 in Fig. 4 falls into a nearly fourfold coordinated site created as the underlying atoms relax either towards or away from the adatom as shown in Fig. 5. Atoms A and B are displaced *towards* the adatom by 0.25 and 0.01 Å, respectively, and atoms C and D are displaced *away from* the adatom by 0.29 and 0.24 Å, respectively. This site

is energetically favored over sites A1 and A2 by 0.13 and 0.07 eV, respectively. (A barely stable fourfold site is also observed at the straight B-type edge and is responsible for the slight minimum between sites 2 and 3 in Fig. 2.) The minimum energy path obtained from the NEB method for descent of an adatom placed initially at either A1 or A2 shows that the adatom first hops to the fourfold site before the exchange descent takes place. The energy along the minimum energy path for an adatom starting in site A1 shows a triple barrier, as the adatom first hops to site A2, then to the fourfold-coordinated site A3, and finally undergoes exchange with the kink atom (see Fig. 6). The barrier for hopping from A2 to the fourfold-coordinated site is small, ~ 0.04 eV. Once the adatom is in site A3, it undergoes the exchange descent, for which the barrier is surprisingly low, only 0.08 eV [37] (with respect to the energy at A3). This energy barrier is similar to the very low diffusion barrier for an adatom on the flat terrace. Here the atom at the end of the truncated row of edge atoms at the kink site provides added coordination which facilitates the exchange descent process.

A kink on a type B edge, however, provides a very different situation. We find higher exchange descent barriers for the type B kink site, higher even than for exchange from the straight type B edge. Here the edge atoms most easily move directly away from the edge, in a direction normal to the step edge. While the end atom of the truncated row provides increased coordination facilitating the exchange descent as at the A-type kink, the end atom also blocks the corner atom at the B-type kink from moving normal to the step edge (see Fig. 7). The net result is a higher descent barrier than at the straight edge. The

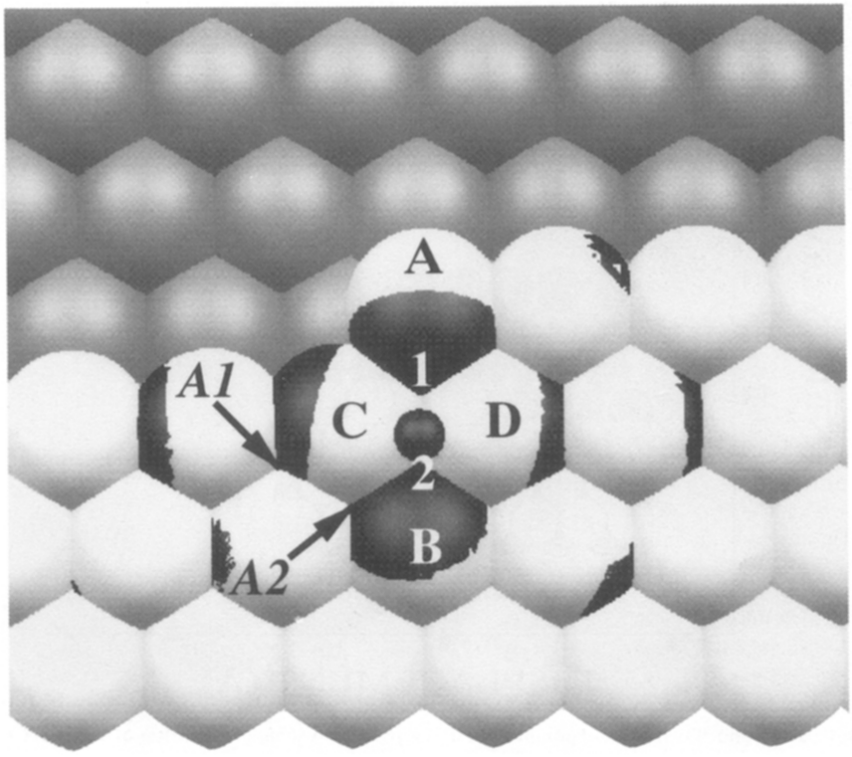

Fig. 5. Displacement of atoms in forming a fourfold-coordinated site at a type A kink. Initial positions with no atom atop are indicated in white, and minimum energy positions when adatom is present atop are indicated in black. The radius for the adatom atop has been reduced to allow a more complete view of displacements for underlying atoms. Configurations with an adatom placed initially in either position 1 or 2 and then relaxed to minimum energy result in near fourfold-coordination of the adatom as underlying atoms A and B relax towards and C and D relax away from the adatom.

minimum energy path for descent of adatoms initially in positions B1 and B3 involves first a hop into position B2 before descent occurs (see Fig. 4). This allows the kink atom to move outwards while minimizing the amount it must push against the underlying atom and the end atom in the extra row. The barrier for exchange descent from the lowest energy, near fourfold coordinated B3 site is 0.20 eV.

While exchange with the kink atom at a B-type edge does not offer a path for descent with lower activation energy than at the straight B edge, the kink site does open a much lower energy path by exchange with the edge atom adjacent to the corner atom (marked I in Fig. 4). Starting at site B4, the adatom can descend by a path with a very low energy barrier of 0.06 eV. Since the displaced edge atom ends up being only fivefold coordinated (by two edge atoms and three underlying atoms) as compared with the sixfold coordinated atom at the end of the truncated row, this illustrates clearly how weakly correlated the activation barriers for descent are with the energy of the final state. Similar to the descent at a straight B-type edge, the atoms adjacent to atom I relax towards the exchanging adatoms, and thereby provide added coordination in the transition state. When one (or both) of these adjacent atoms is a corner atom, this relaxation can occur more readily, further easing the descent process. This barrier for descent near the B-type kink is lower than the barrier for adatom diffusion along the flat (111) terrace.

These results for exchange descent in the vicinity of kink sites would, therefore, support the hypothesis by Poelsema and coworkers, that descent from irregularly shaped island edges is significantly easier than descent from compact islands with predominantly long, straight edges [2]. An interesting consequence of the different char-

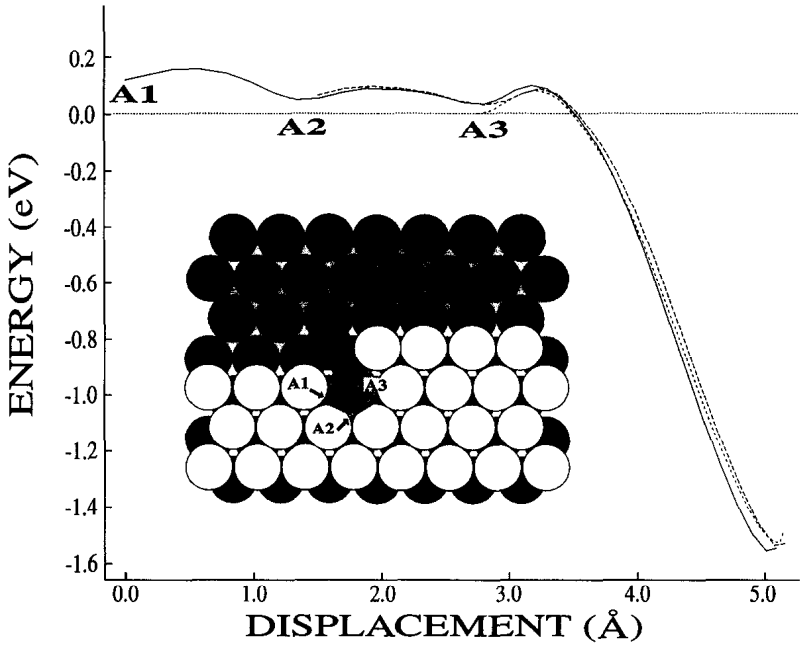

Fig. 6. Potential energy curves and illustration of minimum energy path for exchange diffusion at a type A kink site. Double and triple barriers indicate that an adatom at a type A kink will first hop to the energetically stable fourfold-coordinated site before undergoing exchange with a kink atom. The solid line shows a triple barrier, corresponding to the energy for an adatom starting in A1 to hop through A2 to reach A3 before undergoing exchange with the kink atom. The dashed line shows a double barrier corresponding to the energy of an adatom initially in A2 to move into site A3 before undergoing exchange. The dotted line corresponds to the energy of an adatom initially in A3 to undergo exchange, for which the energy barrier is only 0.08 eV. Final positions for exchanging atoms are lightly shaded.

acter of the two types of edges is that adatoms descending from atop an island will tend to make the B-type edges rough, while A-type edges will tend to grow smooth.

5. Exchange descent from small islands

We have studied exchange descent from atop small, regularly shaped islands and find further evidence to support the barrier-breakdown hypothesis, as activation barriers for adatom descent are much lower for smaller islands. We have studied regularly shaped, compact islands starting with a trimer, a heptamer, and then increasingly larger hexagonal islands consisting of 19 to 169 atoms. For long, straight steps, there is a 0.12 eV difference in the barrier height for exchange descent at the two types of edges. This difference is enhanced as the islands become

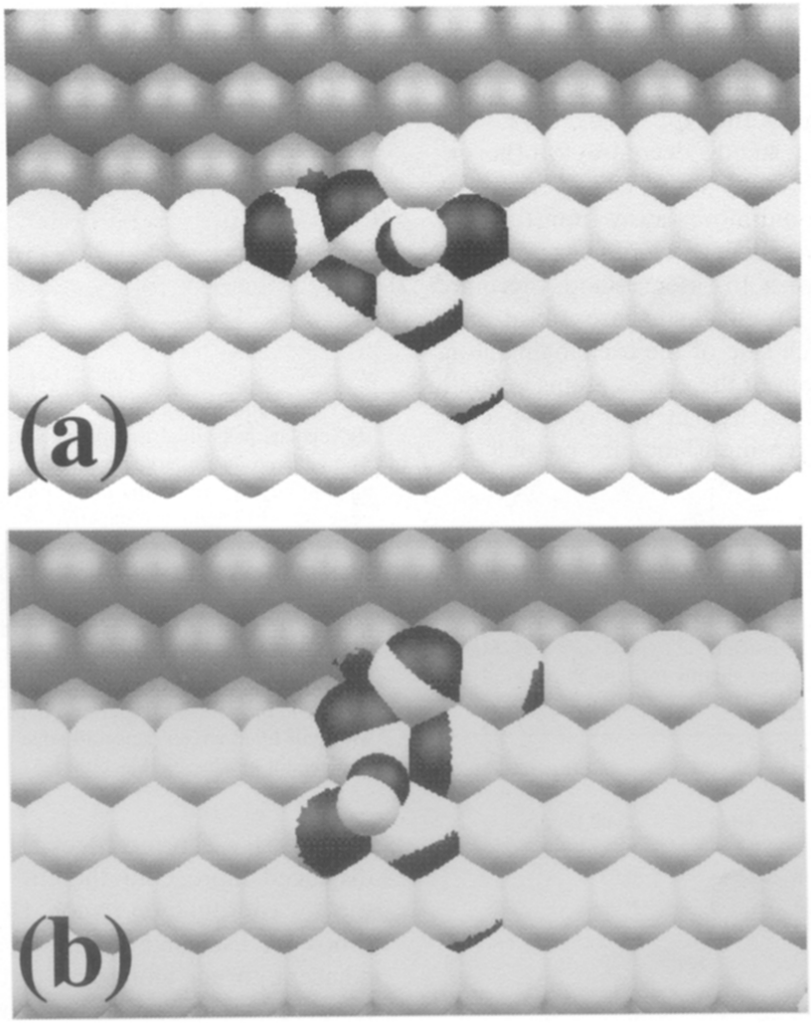

Fig. 7. Same as for Fig. 3 but at kink sites. (a) At a type A kink, the end atom of the truncated row provides increased coordination to the exchanging atoms, facilitating the exchange process. The adatom is displaced sideways because of the underlying atoms. The barrier for descent is 0.08 eV. (b) At a type B kink, the end atom of the truncated row blocks the outgoing edge atom from moving out normal to the straight step in the channel formed by the underlying atoms. It must push against the end atom which in turn pushes on the adjacent edge atom. The exchange diffusion barrier is 0.20 eV, much higher than that for the type A kink or for a straight B-type step. In both (a) and (b) a small displacement in the transition state can be seen by an underlying atom near the kink atom.

smaller; the exchange barrier from the center of the type A step of the island increases while the exchange barrier from the center of the type B step decreases.

Table 2 summarizes the exchange descent barriers found. Fig. 8a shows the initial position for the adatom on top of the larger, hexagonal islands. In each case, the adatom atop starts in the energetically favored edge site at the center of the edge. Fig. 8b shows the cluster-size dependence of the exchange descent barrier. Beginning with a regular 169-atom island and going towards smaller islands, consisting of between 127 atoms to 61 atoms, we see a slight increase in barrier height for exchange at the type A edge. We see a similarly slight but steady decrease for the exchange descent barrier at the type B edge. As the exchanging edge atom moves away from the type A step, it also moves sideways and pushes against adjacent atoms. For a 169-atom island, there are eight atoms along an edge, so there are at least three atoms on each side of the exchanging atom and the displacement of the corner atoms is small. The barrier for exchange at the type A edge increases with decreasing island size possibly because at the shorter edges the corner atoms get displaced more, and thereby pushed more into the low coordination region. However, the barrier drops for exchange at the type B edge because adjacent corner atoms can displace more readily towards the exchanging atoms, facilitating the exchange process.

Comparing 61-atom and 37-atom islands, where there are five and four atoms along an edge, the barrier increases significantly for the type A edge, and drops even more for the type B edge. This trend continues at the B-type edge in

Table 2
Energy barriers for exchange descent from atop compact islands, given for the two types of edges, where the adatom starts in the energetically favored site at the center of the edge; barriers drop dramatically at type-B edge as islands become smaller, but increase slightly for type A edge

Cluster size	Barriers	
Trimer [a]	0.49 eV	
Heptamer [b]	0.48 eV (fcc)	0.29 eV (hcp)
	Type A edge barrier (eV)	Type B edge barrier (eV)
19-atoms	0.38	0.03
37-atoms	0.38	0.06
61-atoms	0.33	0.14
91-atoms	0.32	0.16
127-atoms	0.31	0.17
169-atoms	0.31	0.17
Straight edge	0.30	0.18
Near kink	0.08	0.06

[a] For a trimer, exchange for each atom is equivalent.
[b] For a heptamer, all atoms are corner atoms, so there are no specific type A or B edges. Barriers given for adatom atop initially in an fcc or hcp site.

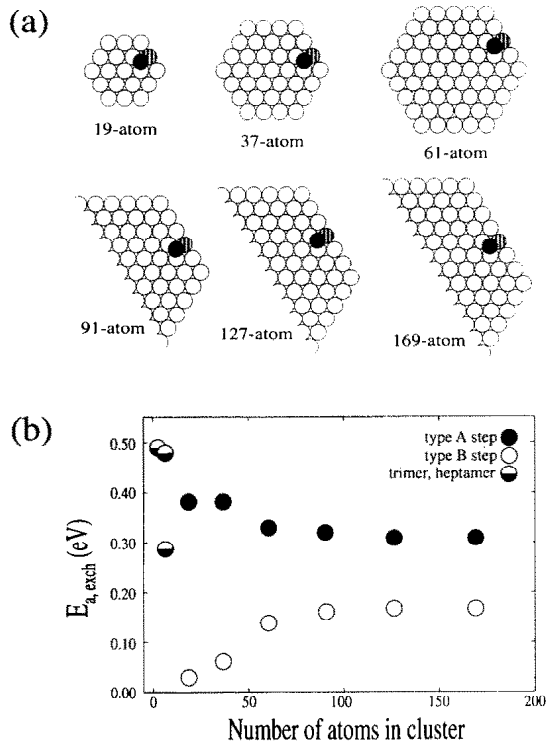

Fig. 8. (a) Illustration of the exchange processes studied for six regular, hexagonal islands consisting of 19 to 169 atoms. The edge atoms undergoing exchange are shown striped. The adatom begins atop in the most central, energetically favored edge site. (b) Island size dependence of the activation energy barrier for exchange descent from the two types of step edges, starting from the site indicated in (a). The barriers for the type A edge are represented with closed circles (●), and those for type B edges are represented with open circles (○). For islands of decreasing size, barriers for the type A edge increase slightly while those for the type B edge fall dramatically. The barriers for trimer and heptamer islands are shown with half-filled circles, since all edge atoms are corner atoms and cannot be classified as either A- or B-type edge atoms.

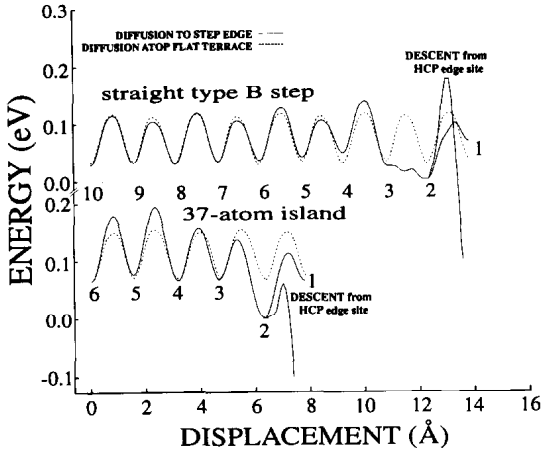

Fig. 9. The solid curves represent the minimum energy path for an adatom to diffuse to a type B edge and then undergo exchange descent at a straight step and from a 37-atom island. The dashed curves (given as a reference) represent the energy for an adatom to diffuse atop a flat terrace. Once an atom finds the energetically favored edge site on a 37-atom island (site 2), the activation barrier for exchange descent (0.06 eV) is considerably smaller than the barrier to return to the center of the island (0.13 eV to hop to site 3). If the adatom starts at site 1, the minimum energy path for descent involves first a hop to site 2 and then exchange with an edge atom.

going to the 19-atom island where both edge atoms adjacent to the displaced atom are corner atoms. There the descent barrier is only 0.03 eV, an order of magnitude lower than for a straight edge. Fig. 9 shows the energy for an atom to diffuse from the center of a 37-atom island to a type B edge and then to undergo exchange. Once an atom hops into the energetically favored edge site (site 2), the activation barrier for exchange descent is considerably smaller than the barrier to return to the island center (0.13 eV to hop to site 3) or the barrier to hop to the adjacent fcc edge site 1 (0.11 eV). Fig. 10 shows the displacement of atoms in the exchange process at the two types of edges on a 37-atom cluster. At the type A edge, the adjacent corner atom is displaced away from and loses coordination with its neighbors, but at the type B edge, the corner atom is displaced towards the exchanging edge atom (by 0.27 and 0.03 Å, respectively), thereby lowering the exchange descent barrier. Using the CEM interaction potential of DePristo and coworkers [38], Wang and Fichthorn calculated the barrier for descent from atop a nine-atom diamond-shaped island [39] and found a barrier of 0.03 eV at the type B edge. This is analogous to the descent from the 19-atom hexagonal island where both atoms adjacent to the displaced edge atom are corner atoms.

To further test the correlation between the

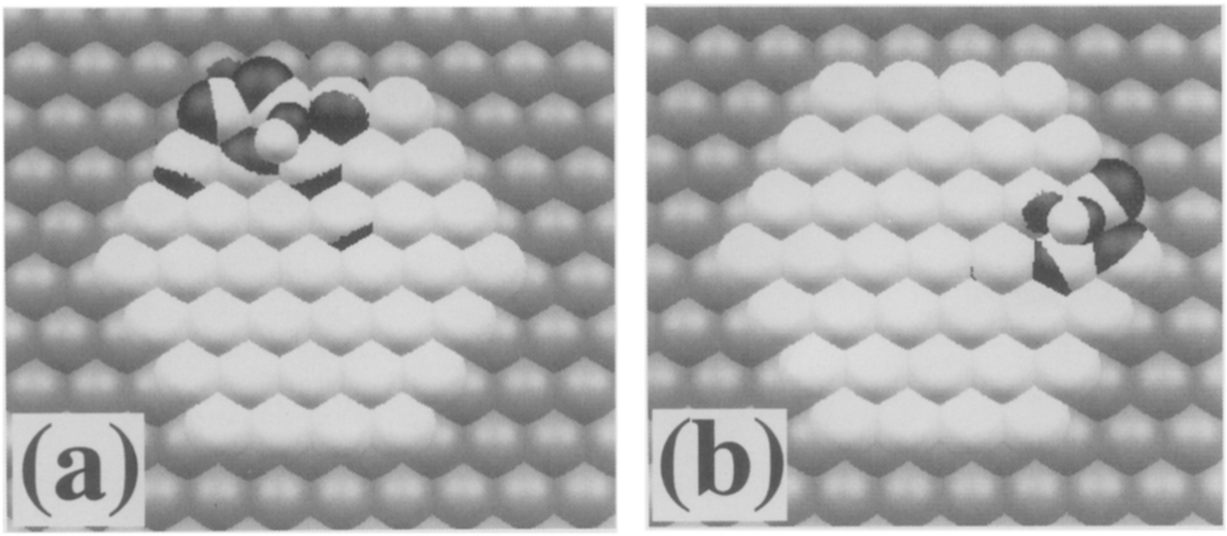

Fig. 10. Same as for Fig. 3 but for exchange descent from 37-atom islands. (a) At the type A step, the exchanging edge atom must push against adjacent edge atoms to move out, resulting in lower coordination for the corner atom and a rise in the exchange descent barrier. (b) At the type B edge, the corner atom adjacent to the exchange process can displace more easily towards the exchanging atoms, further easing the exchange process and leading to an extremely low barrier of 0.06 eV.

descent barrier and the presence of corner atoms, we calculated the barriers for descent by exchange with the edge atom adjacent to a corner atom for all the larger islands, and we obtained similarly low barriers of ~ 0.06 eV at the B-type edges. Although all of these islands can provide very low energy paths for descent, the probability of finding the right site decreases with increasing island size. Table 3 gives a summary of the island size dependence for finding low energy paths for descent. For a 19-atom island, there are three energetically favored edge sites (one for each of the type B edges) which will lead to the very low energy paths for descent. Since there are a total of six energetically favored edge sites, an atom

Table 3
Island size dependence of the abundance of energetically favored edge sites leading to low energy paths for exchange descent (island size is given along with the number of stable edge sites with low energy paths for exchange, the total number of stable (site 2 in Figs. 2 and 9) edge sites, and the ratio of the former with the latter)

Island size	Stable edge sites with low energy paths	Total number of stable edge sites	Ratio (%)
19	3	6	50
37	6	12	50
61	6	18	33
91	6	24	25
127	6	30	20
169	6	36	17

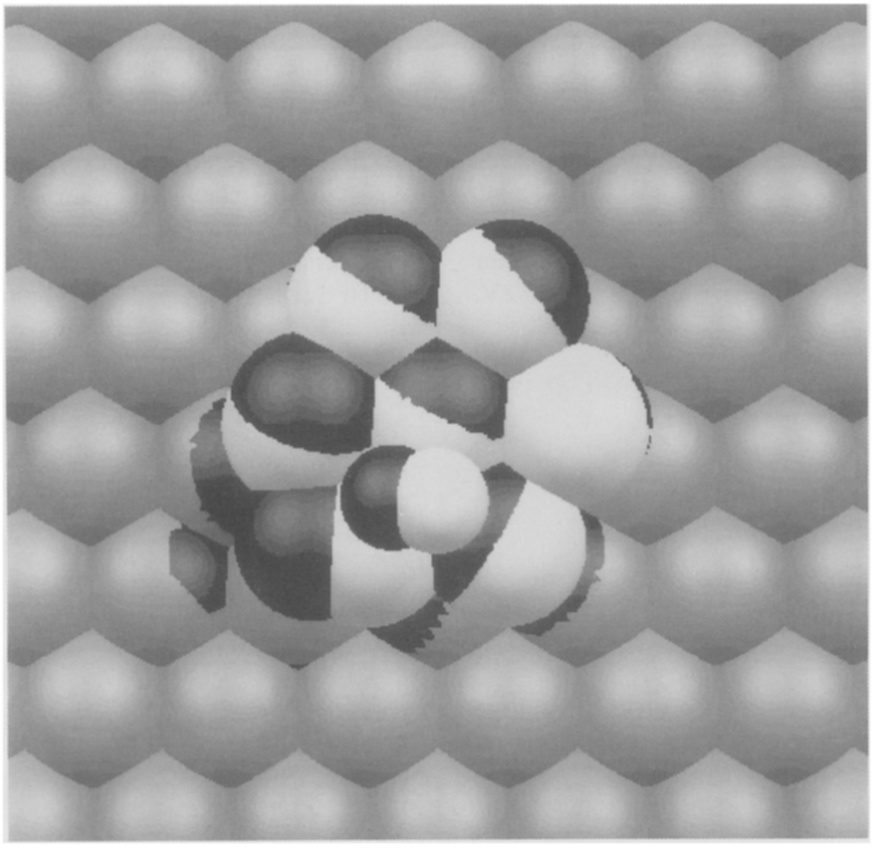

Fig. 11. Same as for Fig. 3 but for exchange descent from a heptamer. Because of its compactness, there is no direct path for the exchanging island atom to move to its new site without greatly reducing coordination with other island atoms. Consequently, it pushes hard against other island atoms to reach its new position, leading to large displacements of all but one of the island atoms and several underlying atoms in the transition state (represented by black spheres). The exchange descent barrier is very high, 0.48 eV.

landing atop a 19-atom cluster has a 50% chance of finding a site leading to a low energy path. Similarly, an atom landing atop a 37-atom island has a 50% chance of finding an edge site with a low energy path for descent. As island size increases, the probability drops down to 17% for a 169-atom cluster. Therefore, although all of these regular, hexagonal islands provide low energy paths for descent, the probability of finding the right initial site is considerably larger for the smaller islands.

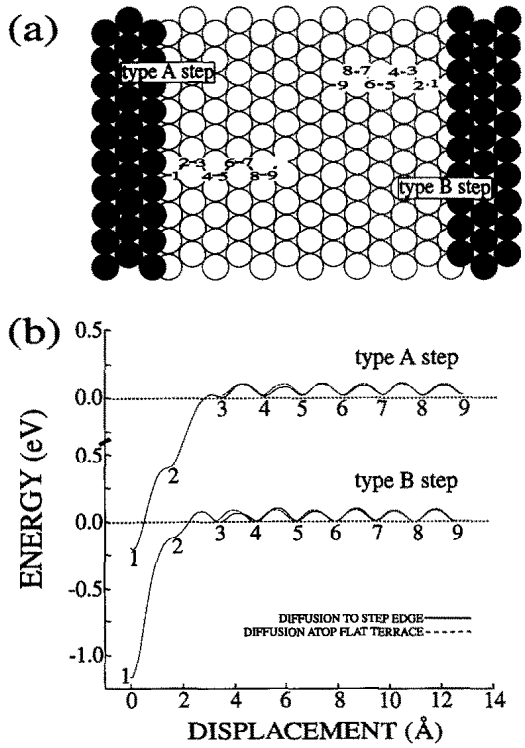

Fig. 12. (a) Illustration of the two types of ascending steps, A and B, with numbered sites corresponding to a general path for an adatom hopping to a step. (b) The dashed curves (given as a reference) correspond to the energy for an atom to diffuse atop a flat terrace. The solid curves represent the minimum-potential-energy profile for an adatom to hop from site 9 to site 1, where an atom in site 1 has twofold coordination with step-atoms. Site 2 is stable at the A-type step, but the barrier for to hop to site 1 is extremely low (< 0.01 eV). Site 2 is unstable for the B-type step, and an adatom hops directly from site 3 to site 1. Reduced barriers from about site 5 to site 1 for both edges would allow adatoms in this region to diffuse more rapidly towards a step.

Very small islands with only corner atoms at the edge are an exception from the trend described above. Specifically, we find the heptamer and trimer have much larger barriers for the exchange descent than even straight edges. For these very small islands, there is no direct path for the displaced edge atom to move without severely losing coordination with the other cluster atoms. The displacement of atoms during exchange descent from atop a heptamer (see Fig. 11) shows how the process causes most of the cluster atoms to be displaced. The energy barrier is 0.48 eV, much higher than at a straight edge. Using the EMT description of the atomic interaction, Stoltze and Nørskov find similarly high barriers for exchange descent from a trimer and a heptamer of Cu on Cu(111) [12]. Consequently, they argued against the barrier-breakdown hypothesis. However, these very small islands where all edge atoms are corner atoms are an exception from a more general trend. Our results for small hexagonal islands consisting of 19 or more atoms confirm that descent barriers for type B edges are in fact much smaller for smaller islands, consistent with the barrier-breakdown hypothesis. The fact that adatoms preferably descend at B-type edges will contribute to the elimination of these types of edges in small islands and the formation of triangular islands surrounded by straight A-type edges. That is, in fact, the island shape observed in STM experiments at 400 K [4]. These small islands, however, mostly grow by sticking of adatoms coming from the terrace the island sits on. The preference for descent at B-type edges will therefore only be a small but possibly significant perturbation on the shape of the growing island.

6. Diffusion towards ascending and descending steps

6.1. Ascending steps

We have calculated the energy for an atom to approach an ascending step for both type A and B edges and note some interesting characteristics. Fig. 12a gives an illustration of the two kinds of

ascending steps, where the sites (numbered 1–9) correspond to positions on the energy curves plotted in Fig. 12b. The solid curves represent the energy for an atom to approach an ascending step, and as in Figs. 2 and 9, the dashed curves provide as a reference the energy for an atom to diffuse atop a large flat terrace. We find position 1 is much lower in energy than the other sites for both types of steps, as an atom experiences increased coordination with the edge atoms. Site 1 is more stable than site 3 by 1.16 eV for the type A step and by 1.14 eV for the type B step. Site 2 is unstable. When an atom is placed in site 2 of the type B edge and the system is relaxed, the adatom spontaneously slides to site 1. We find that the site 2 is just barely stable for the type A step on the Pt(111) surface with an extremely small (< 0.01 eV) barrier for hopping to site 1. Liu and Adams [20] found similar characteristics in EAM barrier calculations for the Ni(111) surface, where adatoms were not stable one nearest-neighbor-spacing from the ascending step for both type A and B steps.

Wang and Ehrlich [40] have observed in FIM experiments an "empty zone", where they see no adatoms ~ 3 nearest-neighbor spacings around clusters on Ir(111). They attribute this absence of adatoms to lower diffusion barriers near ascending steps, so adatoms close enough to a cluster can migrate more rapidly toward the cluster and become incorporated. We find slightly decreased barriers in going from site 5 to site 4 at the type A step and in going from site 4 to site 3 at the type B step. Our results also indicate that once an atom is at site 3, it can easily hop towards the island and become incorporated at site 1 as a result of the extremely low barriers at the type A edge and the instability of site 2 at the type B edge. Wang and Fichthorn [10] have calculated the energy for an atom to approach an irregularly-shaped trimer and a tetramer and found similarly a lower barrier to hop to a nearest-neighbor site at the edge of a cluster.

6.2. Descending steps

We have observed another interesting phenomenon where atoms, having reached island edges, tend to diffuse along the edge rather than returning to the island centers. Wang and Ehrlich have observed similar behavior experimentally for Ir atoms diffusing atop large clusters in FIM studies on Ir(111) [41]. They see that once an atom reaches the cluster edge, it is trapped there and does not return to the center of the island. The edge sites on both type A and B steps, designated as position 2 in Figs. 2 and 9, of both large and small islands provide larger binding energy for the adatom. For long, straight steps, the hcp type A edge site is energetically favored over central sites by ~ 15 meV, and the fcc type B edge site is energetically favored over central sites by ~ 35 meV. The activation barrier for hopping away from the edge is therefore large (~ 0.14 eV), hindering the migration of atoms from edges to central sites. This attraction of adatoms to edge sites is due to the under-coordination of the edge atoms. In general, the lower the coordination, the stronger the bonding. This effect is included in the EAM formalism through the non-linearity of the embedding function. Relaxation has only a minor effect here. The displacements which result from the addition of the adatom are all less than 5% with respect to the lattice spacings and increase the attraction to the edge sites by only 8% (3 meV) as compared with a rigid substrate.

This attraction to edge sites will be more effective at low temperatures, where adatoms, having reached the edge, do not have sufficient energy to escape and remain trapped there. While descent will be less likely at low temperatures because of the lower probability of thermal fluctuations sufficiently large to bring the system over the activation barrier, the trapping could to some extent counter that trend by leading to increased attempt rate. At intermediate temperatures, where adatoms would have sufficient thermal energy to diffuse away from the edge towards the island center but not enough energy to descend readily, the attempt rate for descent could be significantly lower.

We have carried out molecular dynamics simulations at a finite temperature which clearly illustrate the trapping effect. Initially an adatom is placed at an A-type edge site on a thermally

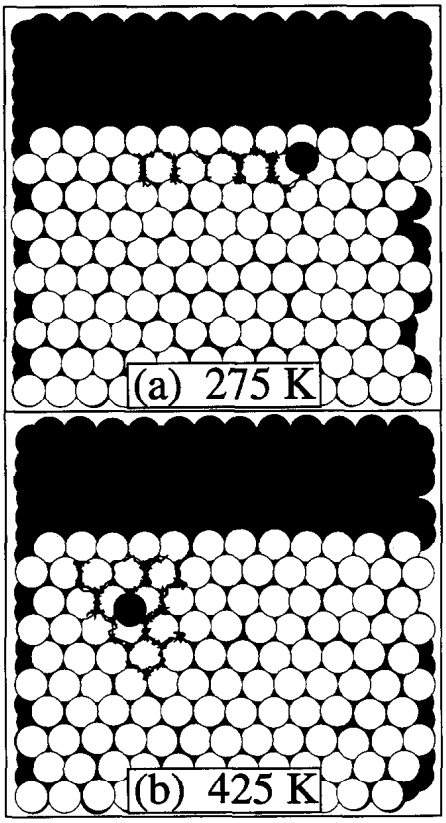

Fig. 13. Trajectories computed by molecular dynamics for an adatom placed by the A type edge of an island at (a) 275 K and (b) 425 K. At the lower temperature the adatom is trapped at the edge and samples *more* edge sites than at the higher temperature.

equilibrated island. Representative trajectories from ten different runs are shown in Fig. 13. After 200 ps, the adatom placed on the colder island (at 275 K) is still at the edge, having visited several edge sites (thereby increasing the chance of finding kink sites leading to low energy paths for descent) while after an equal time interval, the adatom placed on the higher temperature island (at 425 K) has moved away from the edge and has visited fewer edge sites. (In nine out of ten runs at 275 K, the adatom always remained at the edge, at most one nearest-neighbor spacing from the edge. In contrast, only in three out of ten runs at 425 K was the adatom found within ~ 3 nearest-neighbor spacings from the edge after 200 ps. In the remaining seven runs, the adatom had hopped to the interior of the island.) The weak but significant attraction to descending edges could, therefore, contribute to the formation of well-ordered layers at low temperatures but be less effective at intermediate temperature, contributing to reentrant layer-by-layer growth behavior. Other factors need to be taken into account, such as the probability that an adatom ever finds an edge site, to reach a more definitive conclusion about the importance of this effect.

As an adatom approaches the edge sites at a descending step there is a slight decrease in the binding energy (see the energy of sites 7 to 4 in Fig. 2). The rise in the potential energy is particularly sharp (increase of 20 meV) in moving from site 5 to site 4 at the type A edge. The decrease in the binding energy is smaller at the type B edge, amounting to 13 meV when going from site 6 to site 4. The reason for this is a relaxation of the atoms near a step which reduces the interlayer spacing between atoms perpendicular to the edge.

7. Discussion

We can see from the above results that even within the rather simple EAM description of the atomic interactions, activation barriers for descent of adatoms are quite complex. We find a rich variety of barriers even for seemingly similar processes (descent at the two types of edges). One must consider not only the coordination of the exchanging atoms but also the coordination of the adjacent atoms in order to describe an order of magnitude variation of the descent barrier. Simple models that classify these barriers by only counting the bonds formed by the adatom in the initial and final state are likely to overlook important phenomena. It is difficult to comprehend the consequences of the various barriers presented here without carrying out dynamical simulations. These will be the subject of future studies.

Crudely, the temperature at which the system is likely to escape on a given timescale from a given initial state via a transition with a given activation energy can be obtained from the TST approximation, Eq. (1). In vapor deposition, a typical deposition rate is such that the relevant

timescale for diffusive processes is about 1 s. Using a vibrational frequency of 10^{13} s^{-1}, the temperature at which the transition becomes active is $T_a = E_a/30k_B$.

A central issue in understanding the morphology of the surface is the onset of active diffusion of atoms along island edges. Below that temperature, the island edges are likely to be rough, but above that temperature the edges will likely be smooth. Unfortunately, the step edge diffusion barriers have not been measured directly and the EAM estimate is not likely to be reliable, since the analogous channel diffusion barriers on various flat surfaces are not found to agree well with experiment. Our calculated values of 0.60 and 0.43 eV for the A- and B-type edges are likely to be too low. The closest experimental value is the measurement of Bassett and Webber [33] giving 0.69 and 0.84 eV for the (311) and (331) surfaces. Assuming the edge diffusion barriers are ca. 0.8 eV, edge diffusion becomes active at around 300 K. Islands grown at lower temperatures, $T < 300$ K, would be expected to have very irregular shape as atoms come to rest at the site where they first encounter an island edge. Islands grown at higher temperature, $T > 300$ K, would be expected to be more regular in shape with smooth edges, as edge diffusion allows annealing of edge roughness. STM results by Michely and coworkers [4] do indeed show dendritic islands at 200 K and regular, compact islands at 400 K and higher. At 400 K the islands are triangular with A-type edges, but at higher temperatures the shape is nearly hexagonal (at 455 K) and then triangular with mainly B-type edges at 550 K.

Liu et al. [44] have addressed the observed island shapes by carrying out kinetic MC simulations. Using edge diffusion barriers calculated with EMT and slightly modified binding energies, they simulated the growth of islands by sequential addition of atoms and observed the correct triangular shape of islands at the high and low temperature ranges, apparently as a result of kinetic amplification of small differences between the two types of edges. However, their simulations did not result in hexagonal islands in the intermediate temperature range. Instead, the simulated islands were long and narrow, quite different from those observed in STM measurements [4]. The diffusion barriers obtained by EMT [21,43] and reported by Liu et al. are 0.42 and 0.40 eV for type A and B edges, respectively, even lower than the barriers we obtain from the EAM-type potential. The true value of these diffusion barriers and the presence of the triangular and hexagonal islands observed by STM remain open questions and require more work for a clear understanding.

Recently, Šmilauer, Wilby, and Vvedensky [15] carried out MC simulations of Pt crystal growth using a simple bond-counting scheme to predict the diffusion barriers. They were able to reproduce reentrant layer-by-layer growth in qualitative agreement with the experimental measurements [2,3] by building in two effects in the simulation scheme. First, adatoms that land close (within three sites) to an edge experience no barrier to descend. This was interpreted in terms of the push-out effect, where a deposited atom can use its latent heat of condensation to displace peripheral island atoms if directed near an island edge. Second, a significant barrier, was included for adatoms to *approach* a descending step-edge of large compact islands, while there is no barrier for small-irregular islands. Using the EAM-type potential, we find a very small increase in binding energy as an adatom approaches a descending step but not a significant barrier to approach the edge. Furthermore, while we [13] and others [10,12] have observed push-out events in molecular dynamics simulations of low temperature vapor deposition, this effect is probably not of great significance in the experimental situation. Even at the low temperature where the reentrant layer-by-layer growth is observed, islands are too large to have appreciable cross section for push-out. In the case of a heptamer, for which all sites stop are edge sites we have found that only ca. 10% of the impact area leads to push-out (based on 50 runs with random sampling of impact parameters). Push-out is more likely to occur on irregular islands where low energy pathways are present for the exchange process. In our previous MD simulations of Pt vapor deposition at 275 K we found that on average ca. 20% of atoms landing on top of islands were incorporated into the

islands by push-out [13]. Because of extremely fast deposition rate in the simulation, the islands were very small. Larger islands are formed under the experimental conditions, where the flux is much lower. A smaller probability for push-out events would therefore be expected under the experimental conditions than in the simulation. In our MD simulations we found that a greater percentage of deposited atoms landing atop islands descend in thermally-activated exchange processes, mainly at irregular edge sites [13]. Therefore, while the MC simulations of Šmilauer, Wilby, and Vvedensky are able to reproduce the qualitative characteristics of the experimental measurements, the energetics and dynamics calculated using the EAM interaction potential do not support the assumptions on which they base their model.

8. Conclusions

In this paper, we have studied exchange descent processes for a variety of surface configurations using an EAM-type potential to describe the interactions. We find surprisingly low activation energy for exchange descent of adatoms at kink sites and short island edges, an order of magnitude lower than the barrier at long, straight edges. At B-type edges, the important effect is the presence of corner atoms which can easily displace towards the exchanging atoms to increase coordination during the transition and ease the exchange process. At an A-type edge a low energy descent path exists by exchange with the kink atom. As a result, adatoms atop islands with irregular edges can easily descend. STM results at 200 K by Michely and coworkers [4] do indeed show dendritic islands with highly irregular edges in the temperature range where TEAS experiments indicate reentrant layer-by-layer growth [2,3].

We find exchange descent to be most difficult from straight type A steps, more difficult than from type B steps, due to the location of the underlying atoms. Kink sites on A-type edges, however, provide a low energy path for descent, which leads to edge completion and promotes formation of straight A-type edges. STM images taken at 400 K show triangular islands with predominantly straight type A edges [4]. While the preferential descent of adatoms at B-type edges will contribute to greater roughness and faster growth of B-type edges and thereby predominance of A-type edges, this can only be a perturbative effect since most of the atoms in islands at the very low coverage ($\theta \approx 0.1$ ML) where the triangular islands are observed will have arrived from the terrace and stick to the side of the island. It is not clear at this time what exactly determines the shape of the islands. However, given that such triangular islands surrounded by A-type edges are formed at this temperature, the barrier for adatoms to descend from atop the islands is predicted by our calculations to be high enough to significantly impede the interlayer mass transport. Adatoms would be expected to collect and coalesce atop these islands and begin nucleating other islands on which newly deposited atoms can land to repeat the process. This would result in multilayer growth. A monotonic decay indicating 3D growth is indeed seen in the He-atom reflectivity in the temperature range $340 \lesssim T_s \lesssim 450$ K [2,3].

Thus, we have presented results which can help explain the reentrant layer-by-layer growth seen in Pt(111) vapor deposition. Our results strongly support the barrier-breakdown hypothesis of Poelsema and coworkers [2].

An additional effect which may play a role at the lower temperatures, is an attraction of adatoms to descending step edges, which will enhance the probability of descent by increasing the attempt rate and the length of the island perimeter the adatom samples, thereby raising the probability of finding a site leading to a low energy pathway for descent, such as a kink site.

Acknowledgements

We gratefully acknowledge helpful discussions with Bene Poelsema, Thomas Michely and Art Voter. Support for M.V. was provided by the Ford Foundation. International travel funds were provided by the W.W. Stout Fellowship program.

This work has been supported by NSF under Grant No. CHE-9217774 and by The Petroleum Research Fund, administered by the American Chemical Society.

References

[1] M.G. Lagally, Phys. Today November (1993) 24.
[2] B. Poelsema, R. Kunkel, N. Nagel, A.F. Becker, G. Rosenfeld, L.K. Verheij and G. Comsa, Appl. Phys. A. 53 (1991) 369;
R. Kunkel, B. Poelsema, L.K. Verheij and G. Comsa, Phys. Rev. Lett. 65 (1990) 733.
[3] B. Poelsema, A.F. Becker, G. Rosenfeld, R. Kunkel, N. Nagel, L.K. Verheij and G. Comsa, Surf. Sci. 272 (1992) 269.
[4] T. Michely, M. Hohage, M. Bott and G. Comsa, Phys. Rev. Lett. 70 (1993) 3943;
M. Bott, T. Michely and G. Comsa, Surf. Sci. 272 (1992) 161.
[5] A.M. Dabiran, S.K. Nair, H.D. He, K.M. Chen and P.I. Cohen, Surf. Sci. 298 (1993) 384.
[6] W.F. Egelhoff, Jr. and I. Jacob, Phys. Rev. Lett. 62 (1989) 921;
D.K. Flynn, J.W. Evans and P.A. Thiel, J. Vac. Sci. Technol. A 7 (1989) 2162.
[7] S.C. Wang and G. Ehrlich, J. Chem. Phys. 94 (1991) 4071.
[8] D.E. Sanders and A.E. DePristo, Surf. Sci. 254 (1991) 341.
[9] D.E. Sanders, D.M. Halstead and A.E. DePristo, J. Vac. Sci. Technol. A 10 (1992) 1986.
[10] R. Wang and K. Fichthorn, Mol. Simulation 11 (1993) 105.
[11] J.W. Evans, D.E. Sanders, P.A. Thiel and A.E. DePristo, Phys. Rev. B 41 (1990) 5310.
[12] P. Stoltze and J.K. Nørskov, Phys. Rev. B 48 (1993) 5607.
[13] M. Villarba and H. Jónsson, Phys. Rev. B 49 (1994) 2208.
[14] J. Ferrón, Phys. Rev. B 46 (1992) 10457.
[15] P. Šmilauer, M.R. Wilby and D.D. Vvedensky, Phys. Rev. B 47 (1993) 4119.
[16] B. Poelsema, private communication.
[17] H. Jónsson and G. Mills, J. Chem. Phys., submitted.
[18] C.L. Liu, J.M. Cohen, J.B. Adams and A.F. Voter, Surf. Sci. 253 (1991) 334.
[19] G.L. Kellogg and A.F. Voter, Phys. Rev. Lett. 67 (1991) 622.
[20] C.L. Liu and J.B. Adams, Surf. Sci. 262 (1992) 465; 294 (1993) 197.
[21] L. Hansen, P. Stoltze, K.W. Jacobsen and J.K. Nørskov, Phys. Rev. B 44 (1991) 6523.
[22] D.E. Sanders and A.E. DePristo, Surf. Sci. 260 (1992) 116; 264 (1992) L169.
[23] P.J. Feibelman, Phys. Rev. Lett. 65 (1990) 729.
[24] R. Stumpf and M. Scheffler, Phys. Rev. Lett. 72 (1993) 254.
[25] The four different exchange diffusion barriers that have been evaluated with the DFT-LDA method for adatom descent and diffusion along A- and B-type step edges on Al(111) (Ref. [24]) are reproduced to within 0.05 eV in a calculation using EAM-type interaction potential constructed in a way similar to the Pt potential used here; H. Jónsson, unpublished.
[26] W.H. Miller, Acc. Chem. Res. 9 (1976) 306.
[27] D. Chandler, J. Chem. Phys. 68 (1978) 2959.
[28] A.F. Voter and J.D. Doll, J. Chem. Phys. 80 (1984) 5832; J.D. Doll and A.F. Voter, Ann. Rev. Phys. Chem. 38 (1987) 413.
[29] J.M. Cohen and A.F. Voter, J. Chem. Phys. 91 (1989) 5082.
[30] A.F. Voter and S.P. Chen, Mater. Res. Soc. Symp. Proc. 82 (1987) 175.
[31] A. Goldstein and H. Jónsson, unpublished.
[32] J.B. Adams, S.M. Foiles and W.G. Wolfer, J. Mater. Res. 4 (1989) 102.
[33] D.W. Bassett and P.R. Webber, Surf. Sci. 70 (1978) 520.
[34] G.L. Kellogg and P.J. Feibelman, Phys. Rev. Lett. 64 (1990) 3143.
[35] G.L. Kellogg, Surf. Sci. 246 (1991) 31.
[36] We calculate lower diffusion activation energy barriers than reported in Ref. [25] using the same Morse potential parameters presumably because we are including relaxation of more atoms.
[37] In Ref. [13] we reported slightly higher values for descent at A-type steps, 0.32 and 0.11 eV at straight edge and kink site, respectively. These higher values were obtained from calculations using smaller systems and were affected by finite size effects.
[38] T.J. Raeker and A.E. DePristo, Int. Rev. Phys. Chem. 10 (1991) 1.
[39] R. Wang and K.A. Fichthorn, Surf. Sci. 301 (1994) 253.
[40] S.C. Wang and G. Ehrlich, Phys. Rev. Lett. 70 (1993) 41.
[41] S.C. Wang and G. Ehrlich, Phys. Rev. Lett. 67 (1991) 2509.
[42] S.C. Wang and G. Ehrlich, Phys. Rev. Lett. 62 (1989) 2297; 217 (1989) L397.
[43] K.W. Jacobsen, J.K. Nørskov and M.J. Puska, Phys. Rev. B. 35 (1987) 7423.
[44] S. Liu, Z. Zhang, G. Comsa and H. Metiu, Phys. Rev. Lett. 71 (1993) 2967.